

# Position Dependence in the CDMS II ZIP Detectors

V. Mandic\*, W. Rau\*, D. Akerib<sup>†</sup>, P. Brink\*\*, B. Cabrera\*\*, J. P. Castle\*\*, C. Chang\*\*, M. B. Crisler<sup>‡</sup>, D. Driscoll<sup>†</sup>, J. Emes<sup>§</sup>, R. J. Gaitskell<sup>¶</sup>, J. Hellmig\*, S. Kamat<sup>†</sup>, P. Meunier\*, M. Perillo-Issac\*, T. Saab\*\*, B. Sadoulet\*, R. Schnee<sup>†</sup>, D. Seitz\*, G. Wang<sup>†</sup> and B. Young<sup>||</sup>

\*Center for Particle Astrophysics, UC Berkeley, Berkeley, CA 94720, USA

<sup>†</sup>Department of Physics, Case Western Reserve University, Cleveland, OH 44106, USA

\*\*Physics Department, Stanford University, Stanford, CA 94305, USA

<sup>‡</sup>Fermi National Accelerator Laboratory, Batavia, IL 60510, USA

<sup>§</sup>Lawrence Berkeley National Laboratory, Berkeley, CA 94720, USA

<sup>¶</sup>Department of Physics and Astronomy, University College of London, Gower Street, London WC1E 6BT, U.K.

<sup>||</sup>Department of Physics, Santa Clara University, Santa Clara, CA 95053, USA

**Abstract.** The Ge and Si detectors developed by the Cryogenic Dark Matter Search (CDMS) II experiment rely on the simultaneous detection of athermal phonons and ionization produced by interactions in the crystal. The athermal phonons not only provide the total energy deposited during an interaction, but also carry information about the position of the interaction. We describe extracting this information from the pulse shapes in the four phonon sensors arrays. We present the result of measurements made on a Si detector from the first CDMS II production batch. We also investigate ways of using the event position information to extract further information about the phonon signal and about the detector itself.

The ZIP detectors [1, 2, 3] developed by the CDMS collaboration are designed to search for dark matter in the form of Weakly Interacting Massive Particles [4]. We record both the ionization signal and the athermal phonon signal obtained by the Transition-Edge Sensors (TES) in the electrothermal feedback (ETF) mode. In this paper we describe two ways of extracting the event position information, and we use this information to study the phonon signal. We present data collected with a Si ZIP detector exposed to a 12-hole collimator  $^{109}\text{Cd}$  source covering one surface of the detector and a single-hole collimator  $^{241}\text{Am}$  source. Figure 1 (left) shows a drawing of the setup.

The ZIP detectors have 4 phonon sensors (labelled A through D), each covering a quadrant of the Si or Ge crystal. One approach to extracting the event position is to use amplitudes of the four signals, since the largest signal occurs in the primary quadrant (in which the event occurred). We define partitions  $p_x = \frac{(C+D)-(A+B)}{A+B+C+D}$  and  $p_y = \frac{(A+D)-(B+C)}{A+B+C+D}$ , where  $A, B, C, D$  are the pulse amplitudes in the four sensors. Figure 1 (right) shows the event distribution on the detector surface generated by applying this procedure to the Si data. This plot is not a realistic position map - it has a rectangular shape instead of the expected circular one. This is because a part of the phonon signal is lost for events that happen toward the edge of the crystal. Hence, the  $p_y$ - $p_x$  plot folds on itself and the edges

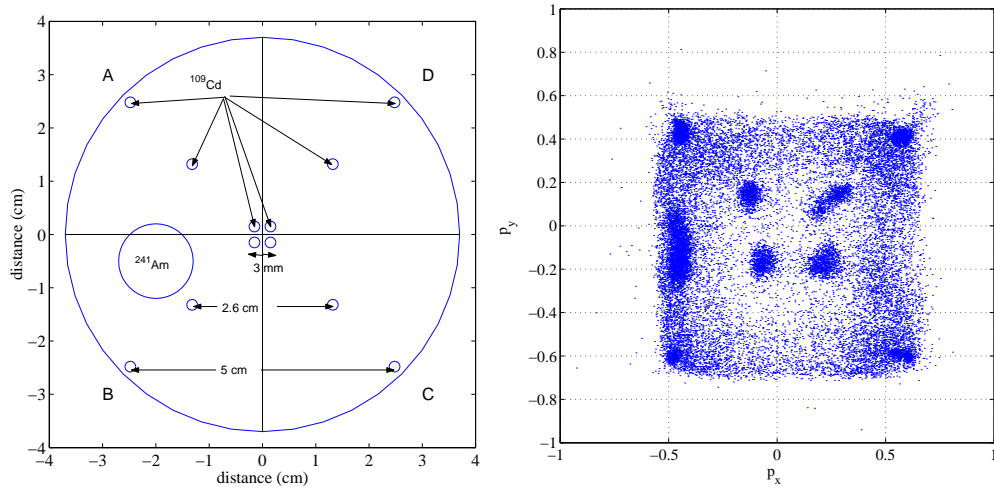


**FIGURE 1.** Left: Schematic of the experimental setup. The outer-most collimator holes are too close to the edge of the crystal and will be discarded in the analysis. Right: Map of the detector surface using phonon partitions.

of the plot are actually formed by the events from the detector interior.

Another approach is to use the delay of the phonon pulses. Since the ionization signal has no delay, the start of the ionization signal is a measurement of the event time. The phonon pulses are delayed with respect to the ionization signal depending on their position. We measure the delay of the 20% of the leading edge of the phonon pulse with respect to the start of the ionization signal. The shortest delay indicates the primary quadrant. Subtracting this shortest delay from the delays of the neighboring sensors gives the  $x$  and  $y$  estimates. The result of applying this algorithm to the Si data is shown in Figure 2 (left). Although this plot does not “fold on itself” and it is a more realistic map of the detector surface, it is not free of non-linearities. In particular, the inner four Cd blobs in this plot correspond to collimator holes that are 0.3 cm apart, while the outer four are 2.6 cm apart. Hence, the position resolution of this map is the best in the center of the detector and it worsens toward the edge. The magnitude of this non-linearity can be seen in the Figure 2 (right), where we used the physical position of the Cd collimator holes to radially transform the delay  $x$ - $y$  plot into a “physical”  $x$ - $y$  plot. In the corrected plot, the Cd blobs are stretched in the radial direction, but they are centered appropriately. This suggests that two blobs per sensor are not sufficient to fully understand the non-linearity of the delay  $x$ - $y$  plot. Hence, we intend to complement our study using a larger number of point sources.

Although much can be done to improve the understanding of the delay  $x$ - $y$  plot, we can attempt to use the Figure 2 (right) to study the phonon signal position dependence. One interesting result is that the position information is preserved in the phonon signal for a long time after the interaction. Figure 3 (left) compares the signals in sensors A and C for a 100 keV event from the central region of sensor A. The sensor A signal remains larger for at least 2 ms after the event interaction. This observation is surprising because the athermal phonons produced during an interaction become ballistic very quickly due to the anharmonic decay, and are expected to lose the position information after several

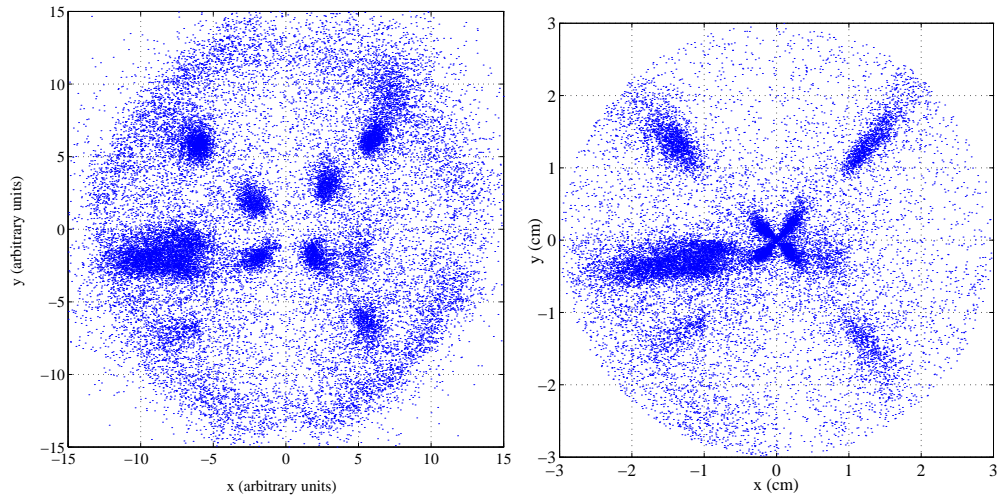


**FIGURE 2.** Left: Delay x-y plot. Right: Physical x-y plot, obtained using the delay x-y plot and the physical positions of the Cd collimator holes. Due to the low resolution, only events within 3 cm from the center will be considered in this study.

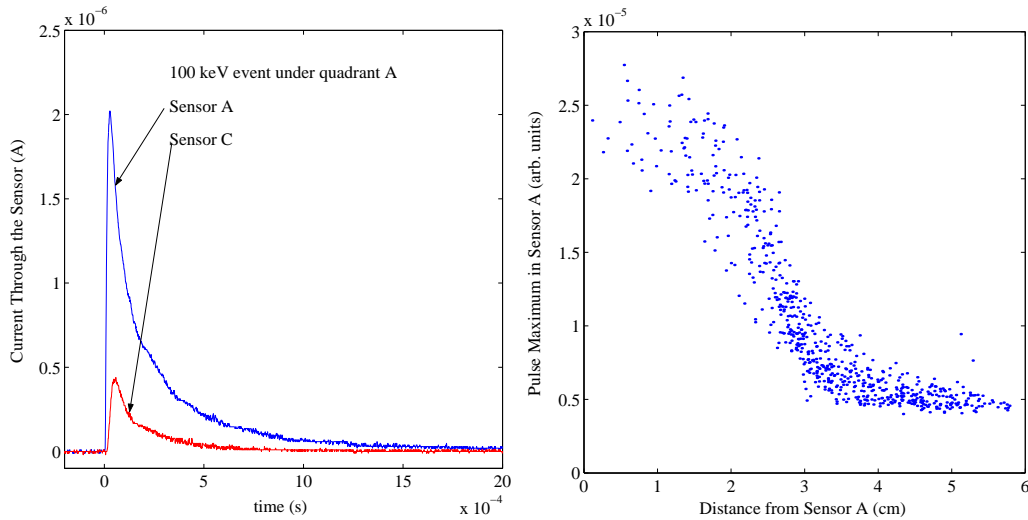


**FIGURE 3.** Left: Comparison of the pulses in sensors A and C for a 100 keV quadrant A event. Right: Pulse maximum in the sensor A (for 150 keV events) as a function of distance from the point  $(-2, 2)$  cm.

bounces off of the crystal surface. Possible explanations, such as secondary phonon production mechanism or TES saturation, are subjects of future studies.

One can also examine the variation of the pulse amplitude as a function of event position. Since each phonon sensor consists of 1008 TES's in parallel, we can only establish an "average" dependence. We define the distance from the sensor A to be the distance from the point  $(-2, 2)$  cm in Figure 2 (right). Figure 3 (right) shows that the largest variation of the pulse amplitude occurs at the boundaries between sensors.

The phonon pulse shape can be further studied by examining the rise and fall times.

The rise-time (important for background rejection in dark matter runs [5]) is determined as the time between the 20% and the 60% of the leading edge. Figure 4 (left) shows the dependence of the rise-time of the sensor A pulses on the distance from the sensor A. Clearly, the rise-time does not vary significantly inside the primary quadrant, but it changes significantly outside of it.

A single exponential fall-time is not sufficient to fit the pulses well. We achieved better fit to the real pulses with  $f(t) = A(e^{-t/\tau_2} - e^{-t/\tau_1}) + B(e^{-t/\tau_4} - e^{-(t-t_0)/\tau_3})$ . The idea is that the first term captures the rise-time and the peak, while the second captures the deviation from the single exponential decay. Some of the parameters (such as  $t_0$  or  $\tau_3$ ) are difficult to estimate reliably and may have no physical meaning. However,  $\tau_4$  captures the fall-time in the tail of the pulse, so it can be estimated easily. Figure 4 (right) shows that  $\tau_4$  depends very weakly (if at all) on the distance from the sensor.

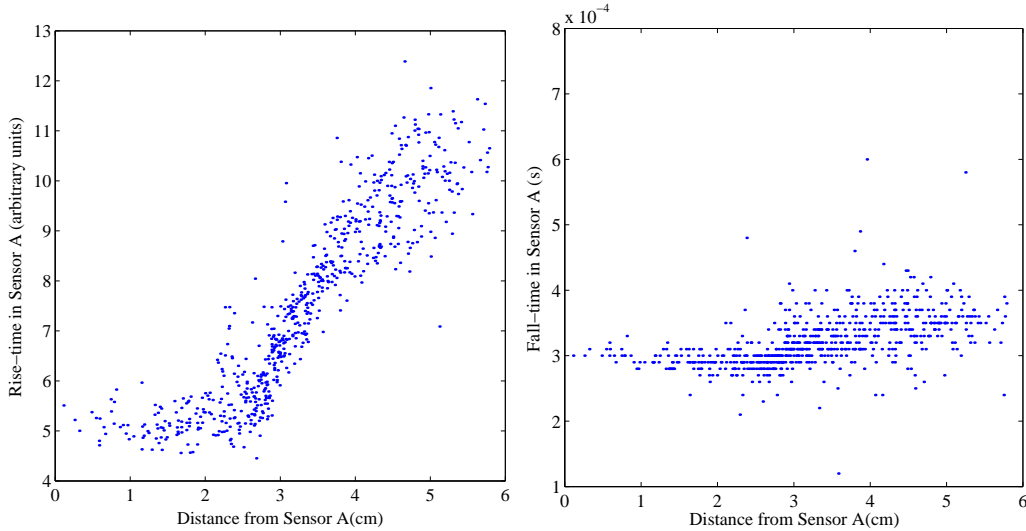


**FIGURE 4.** Left: Dependence of the pulse rise-time on the distance from point  $(-2,2)$  cm. Right: Dependence of the fall-time on the distance from point  $(-2,2)$  cm.

The study we described above will continue. In particular, our goals are to understand better the non-linearities of the delay  $x$ - $y$  plot and to understand the cause of the phonon signal behavior at the millisecond time scales. This work is supported by the Center for Particle Astrophysics, an NSF Science and Technology Center operated by the UC Berkeley, under Cooperative Agreement No. AST-91-20005, by the National Science Foundation under Grant No. PHY-9722414, and by the Department of Energy under contracts DE-AC03-76SF00098, DE-FG03-90ER40569, and DE-FG03-91ER40618.

## REFERENCES

1. T. Saab *et al.*, Nucl. Instrum. Methods A **444**, 300 (2000).
2. B. Cabrera, Nucl. Instrum. Methods A **444**, 304 (2000).
3. J. Hellmig *et al.*, Nucl. Instrum. Methods A **444**, 308 (2000).
4. R. Abusaidi *et al.*, Phys. Rev. Lett. **84**, 5699 (2000).
5. R. M. Clarke *et al.*, Appl. Phys. Lett. **76**, 2958 (2000).